TÜBİTAK

Turkish Journal of Physics

http://journals.tubitak.gov.tr/physics/

Research Article

Turk J Phys
(2016) 40: 150 – 162
© TÜBİTAK
doi:10.3906/fiz-1505-7

The observational status of simple inflationary models: an update

Nobuchika OKADA[1], **Vedat Nefer ŞENOĞUZ**[2,*], **Qaisar SHAFI**[3]
[1]Department of Physics and Astronomy, University of Alabama, Tuscaloosa, AL, USA
[2]Department of Physics, Mimar Sinan Fine Arts University, Şişli, İstanbul, Turkey
[3]Bartol Research Institute, Department of Physics and Astronomy, University of Delaware, Newark, DE, USA

Received: 14.05.2015 • **Accepted/Published Online:** 05.06.2015 • **Final Version:** 27.04.2016

Abstract: We provide an update on five relatively well-motivated inflationary models in which the inflaton is a Standard Model singlet scalar field. These include i) the textbook quadratic and quartic potential models but with additional couplings of the inflaton to fermions and bosons, which enable reheating and also modify the naive predictions for the scalar spectral index n_s and r, ii) models with Higgs and Coleman–Weinberg potentials, and finally iii) a quartic potential model with nonminimal coupling of the inflaton to gravity. For n_s values close to 0.96, as determined by the WMAP9 and Planck experiments, most of the considered models predict $r \gtrsim 0.02$. The running of the scalar spectral index, quantified by $|\mathrm{d}n_s/\mathrm{d}\ln k|$, is predicted in these models to be of order 10^{-4}–10^{-3}.

Key words: Physics of the early universe, inflation

1. Introduction

The dramatic announcement of a B-mode polarization signal possibly due to inflationary gravitational waves by the BICEP2 experiment [1] brought new attention to a class of inflationary models in which the energy scale during inflation is on the order of 10^{16} GeV. Subsequent results by the Planck experiment [2, 3, 4] and the joint Planck–BICEP analysis [5] indicate that most (if not all) of the signal observed by the BICEP experiment was caused by galactic dust. However, a significant contribution from inflationary gravitational waves is not ruled out. The joint Planck–BICEP analysis provides a best fit value around 0.05 for the tensor to scalar ratio r. Although this result is not statistically significant as it stands, it will soon be tested by forthcoming data.

Motivated by these rapid developments in the observational front, in this paper we briefly review and update the results of five closely related, well-motivated, and previously studied inflationary models consistent with values of r around 0.05, a signal level that will soon be probed. The first two models employ the very well-known quadratic (ϕ^2) and quartic (ϕ^4) potentials [6], supplemented in our case by additional couplings of the inflaton ϕ to fermions and/or scalars, so that reheating becomes possible. These new interactions have previously been shown [7, 8, 9] to significantly modify the predictions for the scalar spectral index n_s and r in the absence of these new interactions.

The next two models exploit respectively the Higgs potential [8, 9, 10, 11, 12, 13, 14] and Coleman–Weinberg potential [13, 15, 16, 17]. With the SM electroweak symmetry presumably broken by a Higgs potential, it seems natural to think that nature may have utilized the latter (or the closely related Coleman–Weinberg

*Correspondence: nefer.senoguz@msgsu.edu.tr

potential) to also implement inflation, albeit with a SM singlet scalar field.

Finally, we consider a class of models [18, 19] that invokes a quartic potential for the inflaton field, supplemented by an additional nonminimal coupling of the inflaton field to gravity [9, 20, 21, 22, 23, 24, 25, 26, 27, 28, 29, 30].

Our results show that the predictions for n_s and r from these models are generally in good agreement with the BICEP2, Planck, and WMAP9 measurements, except the radiatively corrected quartic potential, which is ruled out by the current data. We display the range of r values allowed in these models that are consistent with n_s being close to 0.96. Finally, we present the predictions for $|\mathrm{d}n_s/\mathrm{d}\ln k|$, which turn out to be of order 10^{-4}–10^{-3}.

Before we discuss the models, let us recall the basic equations used to calculate the inflationary parameters. The slow-roll parameters may be defined as (see ref. [31] for a review and references):

$$\epsilon = \frac{1}{2}\left(\frac{V'}{V}\right)^2, \quad \eta = \frac{V''}{V}, \quad \zeta^2 = \frac{V'V'''}{V^2}. \tag{1.1}$$

Here and below we use units $m_P = 2.4 \times 10^{18}$ GeV $= 1$, and primes denote derivatives with respect to the inflaton field ϕ. The spectral index n_s, the tensor to scalar ratio r, and the running of the spectral index $\alpha \equiv \mathrm{d}n_s/\mathrm{d}\ln k$ are given in the slow-roll approximation by

$$n_s = 1 - 6\epsilon + 2\eta, \quad r = 16\epsilon, \quad \alpha = 16\epsilon\eta - 24\epsilon^2 - 2\zeta^2. \tag{1.2}$$

The amplitude of the curvature perturbation $\Delta_{\mathcal{R}}$ is given by

$$\Delta_{\mathcal{R}} = \frac{1}{2\sqrt{3}\pi}\frac{V^{3/2}}{|V'|}, \tag{1.3}$$

which should satisfy $\Delta^2_{\mathcal{R}} = 2.215 \times 10^{-9}$ from the Planck measurement [32] with the pivot scale chosen at $k_0 = 0.05$ Mpc^{-1}.

The number of e-folds is given by

$$N = \int_{\phi_e}^{\phi_0} \frac{V\mathrm{d}\phi}{V'}, \tag{1.4}$$

where ϕ_0 is the inflaton value at horizon exit of the scale corresponding to k_0, and ϕ_e is the inflaton value at the end of inflation, defined by $\max(\epsilon(\phi_e), |\eta(\phi_e)|, |\zeta^2(\phi_e)|) = 1$. The value of N depends logarithmically on the energy scale during inflation as well as the reheating temperature, and is typically around 50–60.

2. Radiatively corrected quadratic and quartic potentials

Inflation driven by scalar potentials of the type

$$V = \frac{1}{2}m^2\phi^2 + \frac{\lambda}{4!}\phi^4 \tag{2.1}$$

provides a simple realization of an inflationary scenario [6]. However, the inflaton field ϕ must have couplings to 'matter' fields that allow it to make the transition to hot big bang cosmology at the end of inflation. Couplings

such as $(1/2)h\phi\bar{N}N$ or $(1/2)g^2\phi^2\chi^2$ (to a Majorana fermion N and a scalar χ respectively) induce correction terms to the potential that, to leading order, take the Coleman–Weinberg form [33]

$$V_{\rm loop} \simeq -\kappa\phi^4 \ln\left(\frac{\phi}{\mu}\right) . \tag{2.2}$$

Here, μ is a renormalization scale that we set to $\mu = m_P$[1], and $\kappa = (2h^4 - g^4)/(32\pi^2)$ in the one loop approximation.

First, assume that $\lambda \ll m^2/\phi^2$ during inflation, so that inflation is primarily driven by the quadratic ϕ^2 term. In the absence of radiative corrections, this quadratic case of the well-known monomial model [6] predicts

$$n_s = 1 - 2/N\,, \quad r = 8/N\,, \quad \alpha = -2/N^2\,. \tag{2.3}$$

As discussed in ref. [7], when κ is positive there are two solutions for a given κ. The "ϕ^2 solution" approaches the tree level result eq. (2.3) as κ decreases, whereas inflation takes place close to the local maximum for the "hilltop solution", resulting in a strongly tilted red spectrum with suppressed r. As the value of κ is increased, the two branches of solutions approach each other and they meet at $\kappa \simeq 7 \times 10^{-15}$ for $N = 60$. For negative κ values the $\phi^4 \ln\phi$ correction term in the potential leads to predictions similar to those for the quartic potential given by

$$n_s = 1 - 3/N\,, \quad r = 16/N\,, \quad \alpha = -3/N^2\,. \tag{2.4}$$

For each case, we calculate the inflationary predictions scanning over various values of κ, while keeping the number of e-folds fixed. Figure 1 shows the predictions for n_s, r, and α with the number of e-folds $N = 50$ (left curves in each panel) and $N = 60$ (right curves in each panel), along with the Planck results [4]. The values of parameters for selected values of κ are displayed in Table 2.

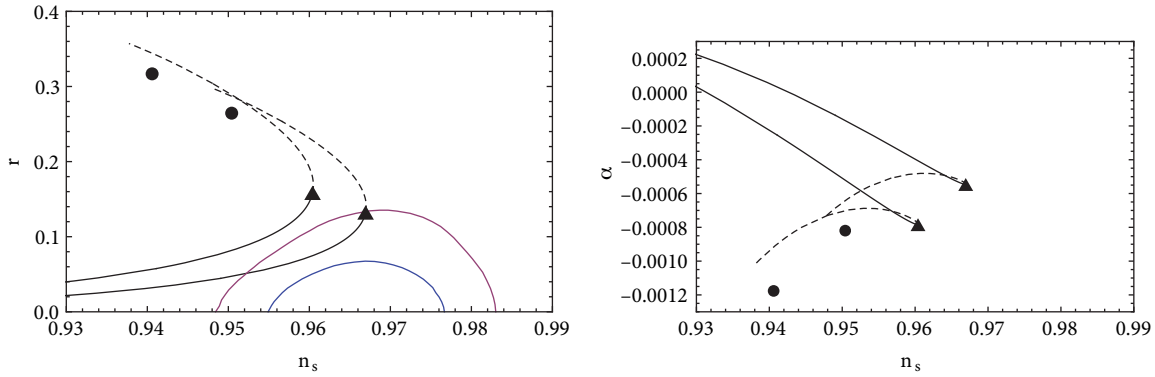

Figure 1. Radiatively corrected ϕ^2 potential: n_s vs. r (left panel) and n_s vs. α (right panel) for various κ values, along with the n_s vs. r contours (at the confidence levels of 68% and 95%) given by the Planck collaboration (Planck TT+lowP) [4]. The black points and triangles are predictions in the textbook quartic and quadratic potential models, respectively. The dashed portions are for $\kappa < 0$. N is taken as 50 (left curves) and 60 (right curves).

The one loop contribution to λ is of order $(4!)\kappa$, which is $\sim m^2/\phi^2$ in the parameter range where the κ term has a significant effect on inflationary observables. In this case our assumption $\lambda \ll m^2/\phi^2$ corresponds

[1]For the radiatively corrected quartic potential the observable inflationary parameters do not depend on the choice of the renormalization scale. However, this may not be the case for the radiatively corrected quadratic potential, as discussed in ref. [34].

Table 1. Radiatively corrected ϕ^2 potential: The values of parameters for number of e-folds $N = 60$, in units $m_P = 1$ unless otherwise stated.

$\log_{10}(\lvert\kappa\rvert)$	m (GeV)	$V(\phi_0)^{1/4}$ (GeV)	ϕ_0	ϕ_e	n_s	r	α (10^{-4})
negative κ branch							
-14.0	1.38×10^{13}	2.23×10^{16}	17.0	1.42	0.962	0.215	-4.81
-14.5	1.46×10^{13}	2.07×10^{16}	16.0	1.41	0.967	0.159	-5.32
-16.0	1.46×10^{13}	1.98×10^{16}	15.6	1.41	0.967	0.133	-5.46
$V = (1/2)m^2\phi^2$							
	1.46×10^{13}	1.98×10^{16}	15.6	1.41	0.967	0.132	-5.46
ϕ^2 branch							
-16.0	1.46×10^{13}	1.97×10^{16}	15.5	1.41	0.967	0.131	-5.47
-14.5	1.41×10^{13}	1.85×10^{16}	15.0	1.41	0.965	0.102	-5.15
-14.3	1.30×10^{13}	1.69×10^{16}	14.4	1.41	0.959	0.070	-3.79
-14.2	1.22×10^{13}	1.59×10^{16}	14.0	1.41	0.954	0.056	-2.59
Hilltop branch							
-14.2	1.01×10^{13}	1.37×10^{16}	13.2	1.41	0.940	0.031	0.58
-14.3	7.9×10^{12}	1.16×10^{16}	12.5	1.41	0.921	0.016	3.41

to the renormalized coupling being small compared to the one loop contribution. Alternatively, assume that $\lambda \gg m^2/\phi^2$ during inflation, so that inflation is primarily driven by the quartic term. The numerical results for this case are displayed in Figure 2 and Table 2. As before, there are two solutions for a given positive value of κ, and the predictions interpolate between a strongly tilted red spectrum with suppressed r to the tree level result given in eq. (2.4). For negative κ values the potential during inflation interpolates between ϕ^4 and $\phi^4 \ln \phi$ potentials, as a consequence the predictions remain close to eq. (2.4).

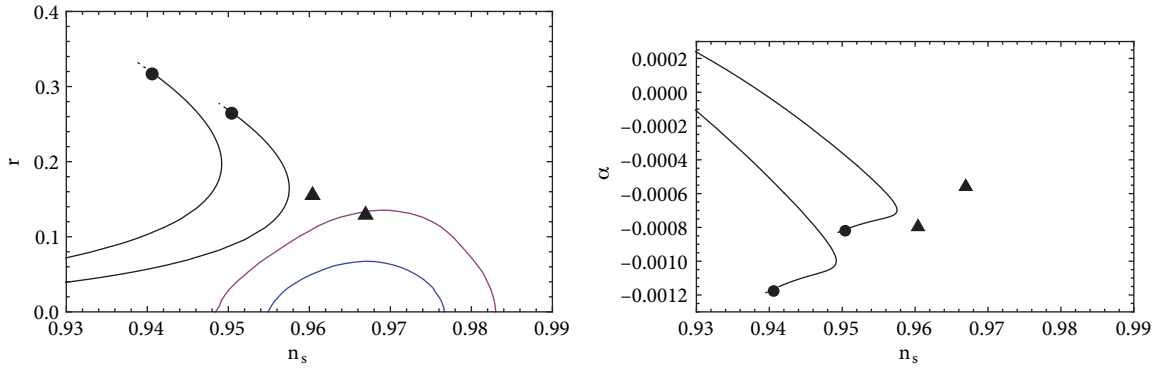

Figure 2. Radiatively corrected ϕ^4 potential: n_s vs. r (left panel) and n_s vs. α (right panel) for various κ values, along with the n_s vs. r contours (at the confidence levels of 68% and 95%) given by the Planck collaboration (Planck TT+lowP) [4]. The black points and triangles are predictions in the textbook quartic and quadratic potential models, respectively. The dashed portions (extending just beyond the black points) are for $\kappa < 0$. N is taken as 50 (left curves) and 60 (right curves).

Table 2. Radiatively corrected ϕ^4 potential: The values of parameters for number of e-foldsl $N = 60$, in units $m_P = 1$ unless otherwise stated.

$\log_{10}(\lvert\kappa\rvert)$	$\log_{10}(\lambda)$	$V(\phi_0)^{1/4}$ (GeV)	ϕ_0	ϕ_e	n_s	r	α (10^{-4})
negative κ branch							
-14.3	-12.4	2.36×10^{16}	22.6	3.67	0.950	0.269	-8.11
-15.0	-12.1	2.34×10^{16}	22.3	3.49	0.951	0.262	-7.97
$V = (1/4!)\lambda\phi^4$							
	-12.1	2.34×10^{16}	22.2	3.46	0.951	0.260	-7.93
ϕ^4 branch							
-15.0	-12.0	2.34×10^{16}	22.1	3.44	0.951	0.258	-7.90
-14.0	-11.8	2.30×10^{16}	21.5	3.28	0.953	0.241	-7.64
-13.5	-11.5	2.17×10^{16}	20.3	3.12	0.957	0.193	-7.23
-13.3	-11.4	1.99×10^{16}	19.1	3.03	0.957	0.135	-6.24
-13.26	-11.3	1.87×10^{16}	18.5	3.00	0.954	0.106	-4.96
Hilltop branch							
-13.26	-11.4	1.70×10^{16}	17.8	2.97	0.947	0.073	-2.28
-13.30	-11.4	1.55×10^{16}	17.2	2.95	0.937	0.051	0.51
-13.35	-11.5	1.44×10^{16}	16.8	2.94	0.929	0.038	2.61

3. Higgs potential

In this section we consider an inflationary scenario with the potential of the form

$$V = \frac{\lambda}{4!}\left(\phi^2 - v^2\right)^2, \tag{3.1}$$

where ϕ is the inflaton field, λ is a real, positive coupling, and v is the vacuum expectation value (VEV) at the minimum of the potential. This Higgs potential was first considered for inflation in refs. [35, 36], and more recently in refs. [9, 10, 13, 15]. Radiative corrections to the Higgs potential were analyzed in refs. [8, 14]. Here, for simplicity, we have assumed that the inflaton is a real field, but it is straightforward to extend the model to the Higgs model, where the inflaton field is the Higgs field and a gauge symmetry is broken by the inflaton VEV.

In the inflationary scenario with the Higgs potential, we can consider two cases for the inflaton VEV during inflation. One is that the initial inflaton VEV is smaller than its VEV at the potential minimum ($\phi_0 < v$), and the other is the case with $\phi_0 > v$. For each case, we calculate the inflationary predictions for various values of the inflaton VEV keeping the number of e-folds fixed. Numerical results are displayed in Table 3. Figure 3 shows the predictions for n_s, r, and α with the number of e-folds $N = 50$ (left curves in each panel) and $N = 60$ (right curves in each panel).

For the case with $\phi_0 < v$, if the inflaton VEV is large ($v \gg 1$ in Planck units) the inflation potential is dominated by the VEV term and well approximated as the quadratic potential

$$V \simeq \left(\frac{\lambda v^2}{6}\right)\chi^2, \tag{3.2}$$

where $\chi = \phi - v$ plays the role of inflaton. Thus the predictions approach the values given by eq. (2.3), corresponding to the black triangles in Figure 3. On the other hand, for $v \ll 1$, the potential is of the new

Table 3. Higgs potential: the values of parameters for number of e-folds $N = 60$, in units $m_P = 1$ unless otherwise stated.

$\log_{10}(\lambda)$	v	$V(\phi_0)^{1/4}$ (GeV)	ϕ_0	ϕ_e	n_s	r	$-\alpha$ (10^{-4})
solutions below the VEV ($\phi < v$)							
-12.3	13	1.18×10^{16}	1.91	11.7	0.947	0.0170	2.67
-12.4	17	1.45×10^{16}	4.64	15.7	0.960	0.0385	4.06
-12.6	23	1.64×10^{16}	9.64	21.7	0.966	0.0626	4.82
-12.9	32	1.76×10^{16}	17.9	30.6	0.968	0.0834	5.14
-13.3	53	1.86×10^{16}	38.3	51.6	0.968	0.104	5.32
-14.9	300	1.96×10^{16}	285	299	0.967	0.128	5.44
solutions above the VEV ($\phi > v$)							
-12.1	1	2.33×10^{16}	22.3	3.69	0.952	0.258	7.85
-12.2	5	2.28×10^{16}	24.3	6.81	0.955	0.237	7.02
-12.5	10	2.22×10^{16}	28.1	11.6	0.959	0.212	6.36
-12.8	19	2.15×10^{16}	36.2	20.5	0.962	0.186	5.91
-13.3	41	2.08×10^{16}	57.4	42.5	0.965	0.161	5.65
-14.9	300	1.99×10^{16}	316	301	0.967	0.137	5.49
$V = (1/2)m^2\phi^2$							
		1.97×10^{16}	15.6	1.41	0.967	0.132	5.46
$V = (1/4!)\lambda\phi^4$							
-12.1		2.34×10^{16}	22.2	3.46	0.951	0.260	7.93

inflation or hilltop type:

$$V \simeq \frac{\lambda}{4!} v^4 \left[1 - 2 \left(\frac{\phi}{v} \right)^2 \right] , \tag{3.3}$$

which implies a strongly red tilted spectrum with suppressed r.

In the other case with $\phi_0 > v$, the inflationary predictions for various values of v are shown as dashed lines in Figure 3. For a small VEV ($v \ll 1$) and $\phi_0 \gg v$, the inflaton potential is well approximated as the quartic potential, and hence the predictions are well approximated by eq. (2.4), corresponding to the black points in Figure 3. On the other hand, for $v \gg 1$ the potential during the observable part of inflation is approximately the quadratic potential, so that the inflationary predictions approach the values given by eq. (2.3) as the inflaton VEV is increased.

4. Coleman–Weinberg potential

In this section we briefly review a class of models that appeared in the early eighties in the framework of nonsupersymmetric GUTs and employed a GUT singlet scalar field ϕ [16, 37, 38, 39]. These (Shafi–Vilenkin) models are based on a Coleman–Weinberg potential [33], which can be expressed as [40, 41, 42]:

$$V(\phi) = A\phi^4 \left[\ln \left(\frac{\phi}{v} \right) - \frac{1}{4} \right] + \frac{Av^4}{4} , \tag{4.1}$$

where v denotes the ϕ VEV at the minimum. Note that $V(\phi = v) = 0$, and the vacuum energy density at the origin is given by $V_0 = Av^4/4$. Inflationary predictions of this potential were recently analyzed in refs. [13, 15, 17].

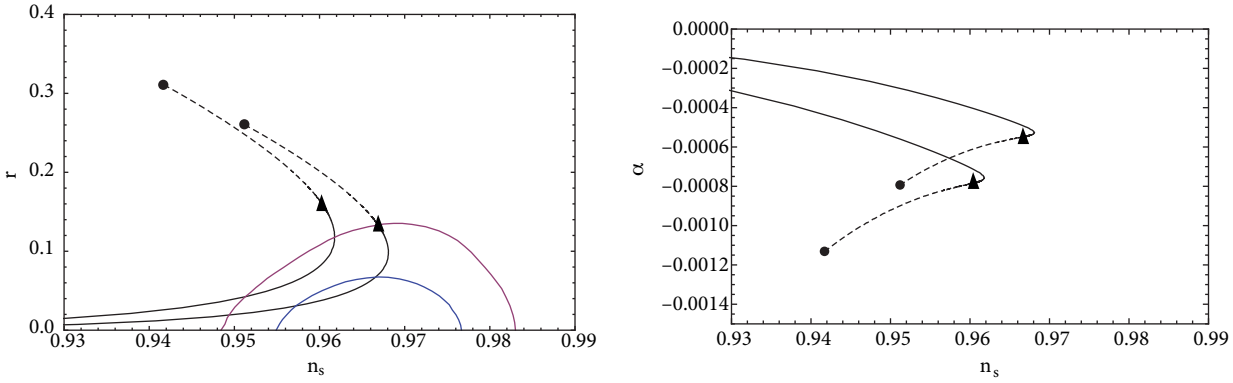

Figure 3. Higgs potential: n_s vs. r (left panel) and n_s vs. α (right panel) for various v values, along with the n_s vs. r contours (at the confidence levels of 68% and 95%) given by the Planck collaboration (Planck TT+lowP) [4]. The dashed portions are for $\phi > v$. The black points and triangles are predictions in the textbook quartic and quadratic potential models, respectively. N is taken as 50 (left curves) and 60 (right curves).

The magnitude of A and the inflationary parameters can be calculated using the standard slow-roll expressions given in Section 1. For $V_0^{1/4} \gtrsim 2 \times 10^{16}$ GeV, observable inflation occurs close to the minimum where the potential is effectively quadratic as in Section 3 ($V \simeq 2Av^2\chi^2$, where $\chi = \phi - v$ denotes the deviation of the field from the minimum). The inflationary predictions are thus approximately given by eq. (2.3).

For $V_0^{1/4} \lesssim 10^{16}$ GeV, assuming inflation takes place with inflaton values below v, the inflationary parameters are similar to those for new inflation models with $V = V_0[1-(\phi/\mu)^4]$: $n_s \simeq 1-(3/N)$, $\alpha \simeq -3/N^2$. We also consider the case where inflation takes place at inflaton values above v (see also [15]), in which case for $V_0^{1/4} \lesssim 10^{16}$ GeV the inflationary parameters are similar to those for the quartic potential given by eq. (2.4).

We display the predictions for n_s, r, and α in Figure 4. The dependence of n_s on V_0 is displayed in Figure 5. Numerical results for selected values of V_0 are displayed in Table 4. Note that in the context of nonsupersymmetric GUTs, $V_0^{1/4}$ is related to the unification scale, and is typically a factor of 3–4 smaller than the superheavy gauge boson masses due to the loop factor in the Coleman–Weinberg potential. For a discussion of inflation in nonsupersymmetric GUTs such as $SU(5)$ and $SO(10)$ with a unification scale of order 10^{16} GeV, see ref. [15]. As discussed in ref. [38], in this class of models it is possible for cosmic topological defects to survive inflation, remaining at an observable level.

5. Quartic potential with nonminimal gravitational coupling

Finally we consider a quartic inflaton potential with a nonminimal gravitational coupling [18, 19, 20]. One of the simplest scenarios of this kind is the so-called Higgs inflation, which has received a fair amount of attention [43, 44, 45, 46, 47, 48, 49, 50, 51, 52, 53]. In Higgs inflation, the SM Higgs field plays the role of inflaton with a strong nonminimal gravitational interaction and a typical prediction is $(n_s, r) = (0.968, 0.003)$ for $N = 60$ e-folds.[2] In nonminimal ϕ^4 inflation, the inflationary predictions vary from those in ϕ^4 inflation (eq. (2.4)) to those in Higgs inflation, depending on the strength of the nongravitational coupling [9, 18, 19, 20]. Nonminimal ϕ^4 inflation

[2]The predictions of SM Higgs inflation depend sensitively on the Higgs and top quark masses, and a larger r value is also possible, see ref. [54, 55] and references therein. For SM Higgs inflation with a nonminimal coupling of the kinetic term, see ref. [56].

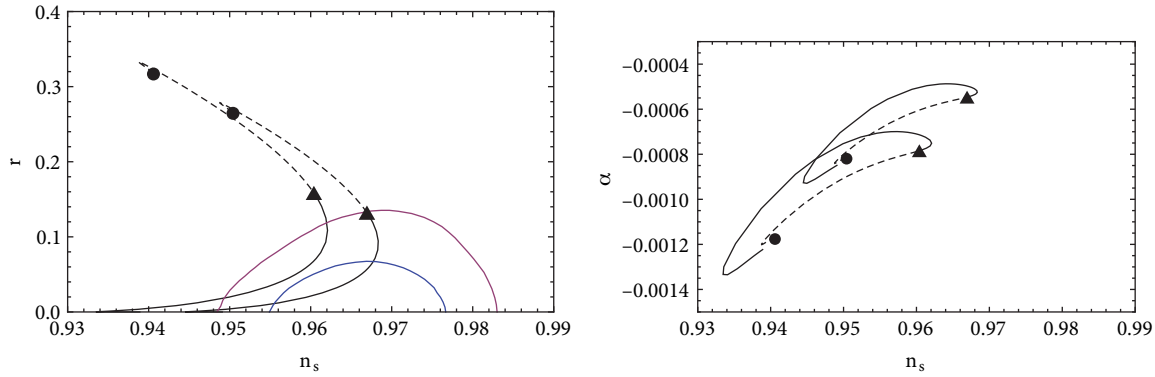

Figure 4. Coleman–Weinberg potential: n_s vs. r (left panel) and n_s vs. α (right panel) for various v values, along with the n_s vs. r contours (at the confidence levels of 68% and 95%) given by the Planck collaboration (Planck TT+lowP) [4]. The dashed portions are for $\phi > v$. The black points and triangles are predictions in the textbook quartic and quadratic potential models, respectively. N is taken as 50 (left curves) and 60 (right curves).

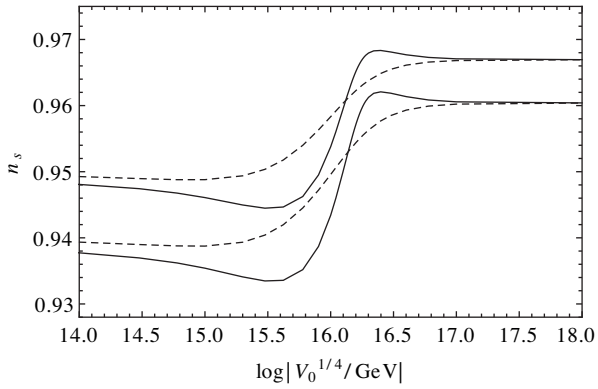

Figure 5. n_s vs. $\log[V_0^{1/4}/\mathrm{GeV}]$ for the Coleman–Weinberg potential. The dashed portions are for $\phi > v$. Top to bottom: $N = 60, 50$.

can be embedded into well-motivated particle physics models [19, 57, 58, 59, 60, 61, 62, 63, 64, 65, 66, 67]. Radiative corrections to the potential have been considered in refs. [9, 18, 19].

The basic action of nonminimal ϕ^4 inflation is given in the Jordan frame

$$S_J^{\mathrm{tree}} = \int d^4x\sqrt{-g}\left[-\left(\frac{1+\xi\phi^2}{2}\right)\mathcal{R} + \frac{1}{2}(\partial\phi)^2 - \frac{\lambda}{4!}\phi^4\right], \tag{5.1}$$

where ϕ is a gauge singlet scalar field, and λ is the self-coupling. We rewrite the action in the Einstein frame as

$$S_E = \int d^4x\sqrt{-g_E}\left[-\frac{1}{2}\mathcal{R}_E + \frac{1}{2}(\partial_E\sigma_E)^2 - V_E(\sigma_E(\phi))\right], \tag{5.2}$$

where the canonically normalized scalar field has a relation to the original scalar field as

$$\left(\frac{d\sigma}{d\phi}\right)^{-2} = \frac{\left(1+\xi\phi^2\right)^2}{1+(6\xi+1)\xi\phi^2}, \tag{5.3}$$

Table 4. Coleman–Weinberg potential: the values of parameters for number of e-folds $N = 60$, in units $m_P = 1$ unless otherwise stated.

$V_0^{1/4}$(GeV)	$V(\phi_0)^{1/4}$(GeV)	$A(10^{-14})$	v	ϕ_0	ϕ_e	n_s	r	$-\alpha(10^{-4})$
solutions below the VEV ($\phi < v$)								
$1. \times 10^{15}$	$1. \times 10^{15}$	1.60	1.63	0.034	0.898	0.946	10^{-6}	9.11
$1. \times 10^{16}$	9.92×10^{15}	4.37	12.7	3.38	11.4	0.954	0.008	5.97
1.5×10^{16}	1.43×10^{16}	2.41	22.1	10.2	20.8	0.964	0.036	4.87
1.75×10^{16}	1.58×10^{16}	1.43	29.4	16.5	28.0	0.967	0.055	4.95
$2. \times 10^{16}$	1.7×10^{16}	0.812	38.7	25.1	37.3	0.968	0.072	5.09
$3. \times 10^{16}$	1.87×10^{16}	0.121	93.4	78.6	92.0	0.968	0.107	5.33
$6. \times 10^{16}$	1.95×10^{16}	0.0059	397.	382.	396.	0.967	0.126	5.43
solutions above the VEV ($\phi > v$)								
$6. \times 10^{16}$	2.00×10^{16}	0.0050	414.	430.	416.	0.967	0.138	5.49
$3. \times 10^{16}$	2.05×10^{16}	0.0623	110.	126.	112.	0.965	0.152	5.57
$2. \times 10^{16}$	2.11×10^{16}	0.215	53.9	70.6	55.4	0.964	0.171	5.70
1.4×10^{16}	2.17×10^{16}	0.496	30.6	48.0	32.2	0.961	0.193	5.93
$1. \times 10^{16}$	2.24×10^{16}	0.847	19.1	37.3	20.7	0.958	0.217	6.30
$6. \times 10^{15}$	2.31×10^{16}	1.29	10.3	29.7	12.1	0.954	0.247	7.02
$1. \times 10^{15}$	2.38×10^{16}	1.20	1.76	23.8	4.64	0.949	0.276	8.24
$1. \times 10^{13}$	2.36×10^{16}	0.50	0.022	22.6	3.67	0.950	0.269	8.10

and the inflation potential in the Einstein frame is

$$V_E(\sigma_E(\phi)) = \frac{\frac{1}{4!}\lambda(t)\phi^4}{\left(1+\xi\,\phi^2\right)^2}. \tag{5.4}$$

The inflationary slow-roll parameters in terms of the original scalar field (ϕ) are expressed as

$$\begin{aligned}
\epsilon(\phi) &= \frac{1}{2}\left(\frac{V_E'}{V_E\sigma'}\right)^2, \\
\eta(\phi) &= \frac{V_E''}{V_E(\sigma')^2} - \frac{V_E'\sigma''}{V_E(\sigma')^3}, \\
\zeta(\phi) &= \left(\frac{V_E'}{V_E\sigma'}\right)\left(\frac{V_E'''}{V_E(\sigma')^3} - 3\frac{V_E''\sigma''}{V_E(\sigma')^4} + 3\frac{V_E'(\sigma'')^2}{V_E(\sigma')^5} - \frac{V_E'\sigma'''}{V_E(\sigma')^4}\right),
\end{aligned} \tag{5.5}$$

where a prime denotes a derivative with respect to ϕ. Accordingly, the number of e-folds is given by

$$N = \frac{1}{\sqrt{2}}\int_{\phi_e}^{\phi_0} \frac{d\phi}{\sqrt{\epsilon(\phi)}}\left(\frac{d\sigma}{d\phi}\right). \tag{5.6}$$

Once the nonminimal coupling ξ and the number of e-folds N are fixed, the inflationary predictions for n_s, r, and α are obtained. Approximate formulas for the predictions of nonminimal ϕ^4 inflation are given

by [18]:

$$n_s \simeq 1 - \frac{3(1+16\,\xi N/3)}{N\,(1+8\,\xi N)}, \tag{5.7}$$

$$r \simeq \frac{16}{N\,(1+8\,\xi N)}, \tag{5.8}$$

$$\alpha \simeq -\frac{3\,\left(1+4\,(8\,\xi N)/3-5\,(8\,\xi N)^2-2\,(8\,\xi N)^3\right)}{N^2\,(1+8\,\xi N)^4}+\frac{r}{2}\left(\frac{16\,r}{3}-(1-n_s)\right). \tag{5.9}$$

The predictions in the textbook quartic potential model are modified in the presence of the nonminimal coupling ξ. For $\xi > 0$, these results exhibit a reduction in the value of r and an increase in the value of n_s, as ξ is increased. Here we have varied ξ along each curve from 0 to $\xi \gg 1$. The numerical results for selected values of ξ are displayed in Table 5. The predicted values of n_s, r, and α are shown in Figure 6 for the number of e-folds $N = 50$ (left curves in each panel) and $N = 60$ (right curves in each panel), along with the n_s vs. r contours given by the Planck collaboration [4].

Table 5. ϕ^4 potential with nonminimal gravitational coupling: the values of parameters for number of e-folds $N = 60$, in units $m_P = 1$ unless otherwise stated.

ξ	$\log_{10}(\lambda)$	$V(\phi_0)^{1/4}$ (GeV)	ϕ_0	ϕ_e	n_s	r	$-\alpha$ (10^{-4})
10^{-5}	-12.1	2.34×10^{16}	22.2	3.46	0.951	0.259	7.93
3.98×10^{-4}	-12.0	2.24×10^{16}	22.2	3.45	0.954	0.218	7.86
0.001	-11.9	2.12×10^{16}	22.2	3.43	0.957	0.174	7.65
0.002	-11.8	1.97×10^{16}	22.1	3.40	0.959	0.131	7.29
0.00398	-11.6	1.79×10^{16}	22.0	3.34	0.962	0.0884	6.79
0.01	-11.3	1.51×10^{16}	21.7	3.18	0.965	0.0451	6.12
1.00	-8.55	0.794×10^{16}	8.52	1.00	0.968	0.00346	5.25
100	-4.62	0.764×10^{16}	0.920	0.107	0.968	0.00297	5.23
$V = (1/4!)\lambda\phi^4$							
	-12.1	2.34×10^{16}	22.2	3.46	0.951	0.260	7.93

6. Conclusion

We have restricted our attention in this paper to models based on relatively simple nonsupersymmetric inflationary potentials involving a SM (or even GUT) singlet scalar field. In the framework of slow-roll inflation, a tensor to scalar ratio $r \sim 0.02$–0.1 for spectral index $n_s \simeq 0.96$ is readily obtained in these well-motivated models. This range of r is of great interest as it is experimentally accessible in the very near future. The running of the spectral index in all these models is predicted to be fairly small, $|\alpha|$ being of order few $\times 10^{-4}$–10^{-3}.

For the Higgs and Coleman–Weinberg potentials, a more precise measurement of r should enable one to ascertain whether the inflaton field was larger or smaller than its VEV during the last 60 or so e-folds (the current data favor the latter). For the quadratic and quartic inflationary potentials we have emphasized, following earlier work, that the well-known predictions for n_s and r can be significantly altered if the inflaton couplings to additional fields, necessarily required for reheating, are taken into account. Despite these radiative corrections, the predictions for the quartic potential are not compatible with the current data. A more precise determination of n_s and r should enable one to also test the radiatively corrected quadratic model.

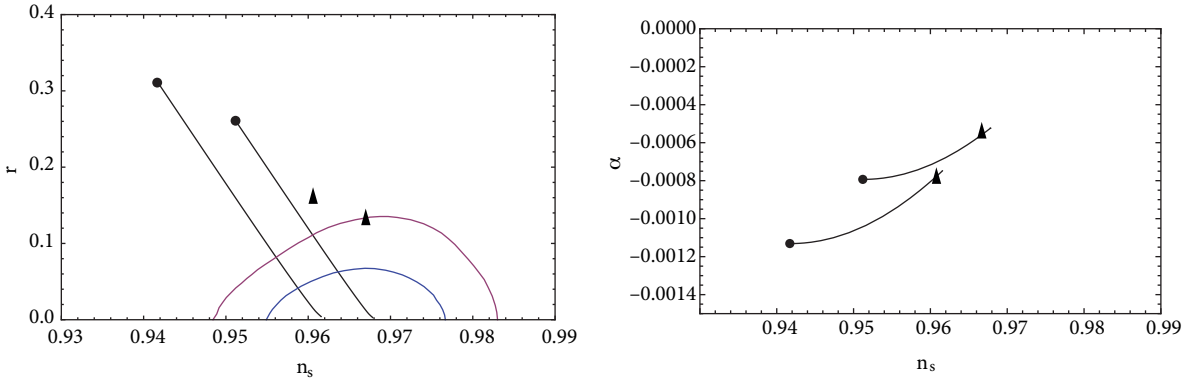

Figure 6. ϕ^4 potential with nonminimal gravitational coupling: n_s vs. r (left panel) and n_s vs. α (right panel) for various ξ values, along with the n_s vs. r contours (at the confidence levels of 68% and 95%) given by the Planck collaboration (Planck TT+lowP) [4]. The black points and triangles are predictions in the textbook quartic and quadratic potential models, respectively. N is taken as 50 (left curves) and 60 (right curves).

We also explored inflation driven by a quartic potential with an additional nonminimal coupling of the inflaton field to gravity. With plausible values for the new dimensionless parameter ξ associated with this coupling, the predictions for n_s and r are in good agreement with the observations.

Acknowledgments

Q.S. acknowledges support provided by the DOE grant No. DE-FG02-12ER41808. We thank Mansoor Ur Rehman for useful comments on the draft version.

References

[1] Ade, P. A. R.; Aikin, R. W.; Barkats, D.; Benton, S. J.;Bischoff, C. A.; Bock, J. J.; Brevik, J. A.; Buder, I.; Bullock, E.; Dowell, C. D.; et al. *Phys. Rev. Lett.* **2014**, *112*, 241101.

[2] Adam, R.; Ade, P. A. R.; Aghanim, N.; Arnaud, M.; Aumont, J.; Baccigalupi, C.; Banday, A. J.; Barreiro, R. B.; Bartlett, J. G.; Bartolo, N.; et al. **2014**, arXiv:1409.5738.

[3] Ade, P. A. R.; Aghanim, N.; Arnaud, M.; Arroja, F.; Ashdown, M.; Aumont, J.; Baccigalupi, C.; Ballardini, M.; Banday, A. J.; Barreiro, R. B.; et al. **2015**, arXiv:1502.02114.

[4] Ade, P. A. R.; Aghanim, N.; Arnaud, M.; Ashdown, M.; Aumont, J.; Baccigalupi, C.; Banday, A. J.; Barreiro, R. B.; Bartlett, J. G.; Bartolo, N.; et al. **2015**, arXiv:1502.01589.

[5] Ade, P. A. R.; Aghanim, N.; Ahmed, Z.; Aikin, R. W.; Alexander, K. D.; Arnaud, M.; Aumont, J.; Baccigalupi, C.; Banday, A. J.; Barkats, D.; et al. *Phys. Rev. Lett.* **2015**, *114*, 101301.

[6] Linde, A. D. *Phys. Lett.* **1983**, *B129*, 177–181.

[7] Senoguz, V. N.; Shafi, Q. *Phys. Lett.* **2008**, *B668*, 6–10.

[8] Rehman, M. U.; Shafi, Q. *Phys. Rev.* **2010**, *D81*, 123525.

[9] Martin, J.; Ringeval, C.; Vennin, V. *Phys. Dark Univ.* **2014**, *5-6*, 75–235.

[10] Destri, C.; de Vega, H. J.; Sanchez, N. *Phys. Rev.* **2008**, *D77*, 043509.

[11] Kallosh, R.; Linde, A. D. *JCAP* **2007**, *0704*, 017.

[12] Kobayashi, T.; Seto, O. *Phys. Rev.* **2014**, *D89*, 103524.

[13] Smith, T. L.; Kamionkowski, M.; Cooray, A. *Phys. Rev.* **2008**, *D78*, 083525.

[14] Okada, N.; Shafi, Q. **2013**, arXiv: 1311.0921.

[15] Rehman, M. U.; Shafi, Q.; Wickman, J. R. *Phys. Rev.* **2008**, *D78*, 123516.

[16] Shafi, Q.; Vilenkin, A. *Phys. Rev. Lett.* **1984**, *52*, 691–694.

[17] Shafi, Q.; Senoguz, V. N. *Phys. Rev.* **2006**, *D73*, 127301.

[18] Okada, N.; Rehman, M. U.; Shafi, Q. *Phys. Rev.* **2010**, *D82*, 043502.

[19] Okada, N.; Rehman, M. U.; Shafi, Q. *Phys. Lett.* **2011**, *B701*, 520–525.

[20] Salopek, D.; Bond, J.; Bardeen, J. M. *Phys. Rev.* **1989**, *D40*, 1753.

[21] Spokoiny, B. *Phys.Lett.* **1984**, *B147*, 39–43.

[22] Futamase, T.; Maeda, K.-I. *Phys. Rev.* **1989**, *D39*, 399–404.

[23] Fakir, R.; Unruh, W. *Phys. Rev.* **1990**, *D41*, 1783–1791.

[24] Kaiser, D. I. *Phys. Rev.* **1995**, *D52*, 4295–4306.

[25] Komatsu, E.; Futamase, T. *Phys.Rev.* **1999**, *D59*, 064029.

[26] Tsujikawa, S.; Gumjudpai, B. *Phys. Rev.* **2004**, *D69*, 123523.

[27] Nozari, K.; Sadatian, S. D. *Mod. Phys. Lett.* **2008**, *A23*, 2933–2945.

[28] Park, S. C.; Yamaguchi, S. *JCAP* **2008**, *0808*, 009.

[29] Kaiser, D. I.; Sfakianakis, E. I. *Phys. Rev. Lett.* **2014**, *112*, 011302.

[30] Tsujikawa, S.; Ohashi, J.; Kuroyanagi, S.; De Felice, A. *Phys. Rev.* **2013**, *D88*, 023529.

[31] Lyth, D. H.; Liddle, A. R. *The Primordial Density Perturbation: Cosmology, Inflation and the Origin of Structure*, Cambridge University Press: Cambridge, UK, 2009.

[32] Ade, P. A. R.; Aghanim, N.; Armitage-Caplan, C.; Arnaud, M.; Ashdown, M.; Atrio-Barandela, F.; Aumont, J.; Baccigalupi, C.; Banday, A. J.; Barreiro, R. B.; et al. *Astron. Astrophys.* **2014**, *571*, A16.

[33] Coleman, S. R.; Weinberg, E. J. *Phys. Rev.* **1973**, *D7*, 1888–1910.

[34] Enqvist, K.; Karciauskas, M. *JCAP* **2014**, *1402*, 034

[35] Vilenkin, A. *Phys. Rev. Lett.* **1994**, *72*, 3137–3140.

[36] Linde, A. D.; Linde, D. A. *Phys. Rev.* **1994**, *D50*, 2456–2468.

[37] Pi, S.-Y. *Phys. Rev. Lett.* **1984**, *52*, 1725–1728.

[38] Shafi, Q.; Vilenkin, A. *Phys. Rev.* **1984**, *D29*, 1870.

[39] Lazarides, G.; Shafi, Q. *Phys. Lett.* **1984**, *B148*, 35.

[40] Albrecht, A.; Brandenberger, R. H. *Phys. Rev.* **1985**, *D31*, 1225.

[41] Albrecht, A.; Brandenberger, R. H.; Matzner, R. *Phys. Rev.* **1985**, *D32*, 1280.

[42] Linde, A. D. *Contemp. Concepts Phys.* **1990**, *5*, 1–362.

[43] Bezrukov, F. L.; Shaposhnikov, M. *Phys. Lett.* **2008**, *B659*, 703–706.

[44] De Simone, A.; Hertzberg, M. P.; Wilczek, F. *Phys. Lett.* **2009**, *B678*, 1–8.

[45] Barvinsky, A.; Kamenshchik, A. Y.; Starobinsky, A. *JCAP* **2008**, *0811*, 021.

[46] Bezrukov, F. L.; Magnin, A.; Shaposhnikov, M. *Phys. Lett.* **2009**, *B675*, 88–92.

[47] Bezrukov, F.; Gorbunov, D.; Shaposhnikov, M. *JCAP* **2009**, *0906*, 029.

[48] Bezrukov, F.; Shaposhnikov, M. *JHEP* **2009**, *0907*, 089.

[49] Barvinsky, A.; Kamenshchik, A. Y.; Kiefer, C.; Starobinsky, A.; Steinwachs, C. *JCAP* **2009**, *0912*, 003.

[50] Barvinsky, A.; Kamenshchik, A. Y.; Kiefer, C.; Starobinsky, A.; Steinwachs, C. *Eur.Phys.J.* **2012**, *C72*, 2219

[51] Clark, T.; Liu, B.; Love, S.; ter Veldhuis, T. *Phys. Rev.* **2009**, *D80*, 075019.

[52] Okada, N.; Rehman, M. U.; Shafi, Q. **2009**, arXiv:0911.5073.

[53] Kamada, K.; Kobayashi, T.; Takahashi, T.; Yamaguchi, M.; Yokoyama, J. *Phys. Rev.* **2012**, *D86*, 023504.

[54] Hamada, Y.; Kawai, H.; Oda, K.-Y.; Park, S. C. *Phys. Rev. Lett.* **2014**, *112*, 241301.

[55] Bezrukov, F.; Shaposhnikov, M. *Phys. Lett.* **2014**, *B734*, 249–254.

[56] Germani, C.; Watanabe, Y.; Wintergerst, N. *JCAP* **2014**, *1412*, 009.

[57] Lerner, R. N.; McDonald, J. *Phys. Rev.* **2009**, *D80*, 123507.

[58] Einhorn, M. B.; Jones, D. T. *JHEP* **2010**, *1003*, 026.

[59] Pallis, C. *Phys. Lett.* **2010**, *B692*, 287–296.

[60] Ferrara, S.; Kallosh, R.; Linde, A.; Marrani, A.; Van Proeyen, A. *Phys. Rev.* **2010**, *D82*, 045003.

[61] Ferrara, S.; Kallosh, R.; Linde, A.; Marrani, A.; Van Proeyen, A. *Phys. Rev.* **2011**, *D83*, 025008.

[62] Okada, N.; Shafi, Q. *Phys. Rev.* **2011**, *D84*, 043533.

[63] Arai, M.; Kawai, S.; Okada, N. *Phys. Rev.* **2011**, *D84*, 123515.

[64] Arai, M.; Kawai, S.; Okada, N. *Phys. Rev.* **2012**, *D86*, 063507.

[65] Arai, M.; Kawai, S.; Okada, N. *Phys. Rev.* **2013**, *D87*, 065009.

[66] Pallis, C.; Toumbas, N. *JCAP* **2011**, *1112*, 002.

[67] Pallis, C.; Shafi, Q. *Phys. Rev.* **2012**, *D86*, 023523.